IEEE Access
Multidisciplinary | Rapid Review | Open Access Journal

Date of publication xxxx 00, 0000, date of current version xxxx 00, 0000.

Digital Object Identifier 10.1109/ACCESS.2017.DOI

Towards Enhancing the Performance of Grid-Tied VSWT Via Adopting Sine Cosine Algorithm-Based Optimal Control Scheme

HUSSEIN SHUTARI [1], NORDIN SAAD [1], (SENIOR MEMBER, IEEE), NURSYARIZAL BIN MOHD NOR [1], MOHAMMAD FARIDUN NAIM TAJUDDIN [2], ALAWI ALQUSHAIBI [3], AND MUAWIA ABDELKAFI MAGZOUB [1],(MEMBER, IEEE)

[1]Department of Electrical and Electronic Engineering, Universiti Teknologi PETRONAS, Seri Iskandar 32610, Malaysia (e-mail: hussein_20000028@utp.edu.my, nordiss@utp.edu.my, nursyarizal_mnor@utp.edu.my, muawia.mohamedali@utp.edu.my)
[2]School of Electrical Systems Engineering, Universiti Malaysia Perlis, 02600 Arau, Perlis, Malaysia (e-mail: faridun@unimap.edu.my)
[3]Department of Computer and Information Sciences, Universiti Teknologi PETRONAS, Seri Iskandar 32610, Malaysia (e-mail: alawi_18000555@utp.edu.my)

Corresponding author: Hussein Shutari (hussein_20000028@utp.edu.my).

This Research was funded by Fundamental Research Grant Project (FRGS) from the Ministry of Education Malaysia (FRGS/1/2019/TK04/UTP/02/10) and the UTP Graduate research assistantship scheme.

ABSTRACT The expanding trend of wind power technology motivates scholars to pursue more investigation on optimising energy extraction from the wind and integrating high-quality power into the utility grid. This paper is aimed at introducing a novel application of the sine cosine algorithm (SCA) which attempts to find the optimal gains of proportional-integral (PI) controllers used to control the power electronic converter (PEC) equipped with the Variable speed Wind turbine (VSWT) such that a maximum power extraction and performance enhancement can be realized. The PEC equipped with the VSWT combines a machine side converter (MSC) and a grid-side inverter (GSI). Both the MSC and GSI are controlled by the proposed SCA-based PI controllers through cascaded vector control schemes. The MSC is responsible for controlling the wind generator's rotational speed, active power, and reactive power. The GSI is used to regulate the dc-link voltage and to keep the terminal voltage at the desired frame set by the operator. To obtain the optimum PI gains, the SCA is applied to minimize the sum of the integral squared error (ISE) of twelve PI controllers error inputs in the control schemes simultaneously. Performances of the proposed SCA-PI control schemes are assessed under severe grid disturbance and random wind speed variation to mimic more realistic conditions. The effectiveness of the proposed SCA-PI is verified in the MATLAB/Simulink environment, and the results are compared to those obtained using a grey wolf optimizer and particle swarm algorithm-based optimal PI controller. The simulation findings confirm the SCA-PI can be regarded as an efficacious way to enhance the performance of the VSWT.

INDEX TERMS Wind turbine control, power electronic converter, MPPT, PMSG, PI controller, sine cosine algorithm.

I. INTRODUCTION

RENEWABLE energy sources such as wind, solar, hydro, and others are widely regarded as promising energy sources for electricity generation [1]. Wind energy has emerged as the most important and more productive energy source for the future. This is owing to its commercial merits, environmentally friendly and frequently large power [2]. In 2020, the installations of new turbines brought the global cumulative wind power capacity up to 743 GW. This reflects an increase of 93 GW above the previous year's record. According to recent estimations, installed wind energy is projected to exceed 917 GW worldwide by 2030 [3]. During the massive expansion of the wind energy industry, many improvements have been made to the wind energy conversion system (WECS) [4]. In WECS, the Wind turbine (WT) is considered a major component of the system. It can be

categorised into variable speed wind turbine (VSWT) and fixed speed wind turbine (FSWT) depending on the wind speeds being handled. The VSWTs have gained interest in the modern wind energy sector. Such growing interest in VSWTs can be related to their distinct characteristics, such as maximum power extraction, less ripple, and full controllability as compare to FSWT [5]. In the wind power sector, different kinds of generators are equipped with VSWT including the permanent magnet synchronous generators (PMSGs) [6], the squirrel cage induction generators (SCIGs) [7], and the doubly-fed induction generators (DFIGs) [8]. Despite the DFIG's economic choice, many key advantages reside behind the extensive use of PMSGs based VSWT. Among the distinguishing advantages of PMSG are self-excitation, gearless construction, operational conditions characterized by high power factor, and density of electrical power [9], [10].

In the general configuration, a VSWT-PMSG is linked to the utility grid (UG) via a fully controlled back-to-back converter (FCBTBC). The FCBTBC consists of two voltage source converters (VSCs) coupled together by a DC-link capacitor. The VSCs are referred as grid side inverter (GSI) and machine side converter (MSC). This configuration has a significant advantage such that the FCBTBC decouples the PMSG from the UG. As a result, grid disruptions/fluctuations do not directly impact the PMSG [11], [12]. In view of the control scheme, both the MSC and the GSI are commonly controlled via a cascaded vector control scheme [13]. The cascaded vector control scheme is usually based on either traditional proportional-integral (PI) controllers, fuzzy logic control (FLC), slide mode control (SMC), or adaptive neural network (ANN). However, in the wind power industry, the use of SMC, FLC, and ANN controllers are limited due to their sophisticated computations [14]–[17].

The PI controllers are still prevalent in many industrial applications thanks to their features, such as simplicity, durability, and wide ranges of stability [18]. Nevertheless, the PI controllers are acutely susceptible to uncertainty, nonlinearity, and parameters variations of the system [19]. Various approaches for properly designing the gains of cascaded PI controllers have been introduced in the literature [20]. Creating such a controller in most of those approaches relied on trial-and-error criteria, which is time-consuming, takes a lot of effort, and is mostly dependent on the designer's competence. As a result, fine-tuning PI controllers pose a significant challenge to control designers, particularly in WECS, where transfer functions or mathematical models are difficult to present. Therefore, many meta-heuristic algorithms have recently been utilized to fine-tune cascaded PI controllers gain for enhancing grid-tied VSWT-PMSG performance [21].

Among examples of the applied algorithms are the gravitational search algorithm [22], augmented grey wolf optimizer [23], water cycle algorithm [24], democratic joint operations algorithm [25], grey wolf optimizer [26], whale optimization algorithm [27], particle swarm optimization algorithm [28], optimal transient search algorithm [29] bacterial foraging optimization [30], symbiotic optimization algorithm [31], and adaptive filtering algorithm [32]. By utilising the aforementioned optimization approaches, significant improvements are genuinely achieved for the grid-connected VSWT-PMSG. However, based on the No free lunch (NFL) theorem, not a particular algorithm can effectively address all types of optimization problems. Therefore, the adoption of a novel meta-heuristic algorithm to optimizing the renewable energy conversion system aiming to get accurate, and satisfactory performance is still growing and blossoming. This constitutes the main incentive to implement a novel algorithm namely sine cosine algorithm (SCA) to fine-tune gains of cascaded PI controllers of a grid-tied VSWT-PMSG.

The SCA is a novel population-based optimization technique that Seyedali Mirjalili created in 2016 [33]. It employs the sine and cosine arithmetic equations to seek the global optimal solutions stochastically. When it comes to applying the SCA to an optimization problem, specific characteristics such as low tuning parameters, high optimization accuracy, powerful global searchability, and fast convergence speed all contribute to its advantages. The SCA has been effectively used in multiple disciplines of optimization problems, involving machine learning [34], image processing [35], power system engineering [36], networking, and others [37].

This paper's contributions are as follows: an investigation of exploring a new approach in which the SCA is employed to optimize controller's gains of two converters involved in enhancing the grid-tied VSWT-PMSG performance. The focus is to have the first controller appropriately controls the converter to efficiently regulate generator rotational speed and produces maximum power extraction and the second controller to optimally controls another converter to regulate the DC-link voltage and the grid currents, under grid disturbance and fluctuating wind speed scenarios. Beside,a new idea of the MPPT algorithm that does require wind speed measurement is used to generated optimal rotational rajectory. The SCA optimisation procedure can directly be applied to the cascaded vector PI controller and select the best gain values based on the minimum fitness function. This can be recognized as simulation-based optimization, which represents a simple, fast, and precise technique. This study selects the Integration square error (ISE) criterion as a fitness function. The SCA optimization results have been evaluated using statical analysis and ANOVA test technique to verify its feasibility.

The modelling and control schemes of the system under consideration are depicted. The SCA-PI control scheme's peformance is evaluated under grid disturbance and fluctuating wind speed scenarios. The effectiveness of the SCA-PI controller is compared to the PI controllers optimized by the PSO algorithm and GWO algorithm. The simulation results via MATLAB/Simulink environment validate the accuracy of the developed control schemes. To the best of the authors' knowledge, the research on a cascaded SCA-PI control scheme for controlling a VSWT-PMSG system has not been reported in the literature related to WECS.

II. CONFIGURATION OF THE WECS

This section outlines the configuration of WECS used in this study. As shown in Figure 1, the WECS is equipped with a VSWT-PMSG and coupled to the UG through an FCBTBC and a filter. The FCBTBC is comprised of an MSC and a GSI that are connected together with an overvoltage-protected capacitor. Moreover, the FCBTBC is associated with three controllers to be referred as MPPT controller, MSC controller and GSI controller. In this configuration, the mechanical power created by aerodynamic forces acting on the WT blades is delivered to the PMSG via a shaft. The PMSG then converts the mechanical power into electrical power. This power is fed into the utility grid via FCBTBC and filtered to meet the grid's requirements.

A. WT MODEL

In WECS, the kinetic wind energy is regarded as a prime mover of a VSWT and is denoted as:

$$P_{wind} = 0.5\rho A V_{\omega}^{3} \tag{1}$$

where ρ represents the density of air (kg/m^3), A denotes the swept region covered by the blades of WT (m^2), and V_{ω} indicates the wind speed (m/s). Based on the Betz limit [38], the WT cannot harness all of the available wind energy. The amount of wind energy that is transferred into mechanical power is computed as in Equation (2) [39].

$$P_m = 0.5\rho A V_{\omega}^{3} C_p(\beta, \lambda) \tag{2}$$

here, C_p is the power coefficient (conversion efficacy). In accordance with the dynamic behaviour of wind turbines, a general equation expressing the power coefficient is as follows:

$$C_p(\beta, \lambda) = 0.22(\frac{116}{\lambda_i} - 0.3\beta - 5)e^{\frac{-12.5}{\lambda_i}} \tag{3}$$

With

$$\frac{1}{\lambda_i} = (\frac{1}{\lambda + 0.08\beta} - \frac{0.035}{\beta^3 + 1}) \tag{4}$$

Referring to Equation (3), two major variables influence C_P: blade angle β, and Tip Speed Ratio (TSR) of the WT blade $\lambda = R\omega_m/V_{\omega}$. Here R is the rotor plane radius and ω_r is the angular speed of the rotor. In this study, it is considered that the pitch angle β is zero (optimal value) as the work focuses on the maximum power extraction region. Consequently, the C_p is solely dependent on λ [40]. At any prevailing wind speed, wind turbines must be rotated at an optimal rotational speed ($\omega_{r.opt}$) which leads to the optimal TSR and the optimal power coefficient $C_{p.opt}$ so as to the maximum wind power is extracted. The WT output power as a function of rotational speed for various wind speeds is presented in Figure 2.

B. PMSG MODEL

The PMSG transforms mechanical energy into electrical energy even at low rotational speeds. It has the advantages of high-electrical power density, reduced copper loss as no field winding, and reasonable cost [41]. The electrical voltages supplied by the PMSG in the rotating reference frame ($dq - axis$) are stated as:

$$v_{ds} = R_s i_{ds} + L_d \frac{di_{ds}}{dt} - \omega_e L_q i_{qs} \tag{5}$$

$$v_{qs} = R_s i_{qs} + L_q \frac{di_{qs}}{dt} + \omega_e \psi_f + \omega_e L_d i_{ds} \tag{6}$$

where i_{ds},i_{qs}, v_{ds} and,v_{qs} are currents and voltages of the PMSG's stator. L_q,L_d are the stator inductances and R_s is the stator resistance. Correspondingly, ψ_f and ω_e represent the magnetic flux and the electrical angular speed respectively. The electrical angular speed ω_m is related to mechanical speed as a function of the number of machine poles p_n is written as below:

$$\omega_e = P_n \omega_m \tag{7}$$

The PMSG electromagnetic torque T_e is expressed by the following:

$$T_e = \frac{3}{2} P_n[(L_d s - L_q s) i_{ds} i_{qs} - \psi_f i_{qs}] \tag{8}$$

Therefore, the dynamic model equation of The PMSG is formulated as Equation (9).

$$J\frac{d\omega_m}{dt} = T_e - T_m - D\omega_m \tag{9}$$

here, J, D and T_m denote the moment of inertia, the generator's rotor damping coefficient and the mechanical torque respectively.

III. CONTROL SCHEMES OF THE FCBTBC

The wind energy captured by the WT is a nonlinear function of its rotational speed. For each wind turbine, at a certain wind speed, there is a unique rotational speed at which the extracted power is maximized [42]. Therefore, the WT needs to be operated at an optimum rotational speed related to the wind speed. In addition, the generated wind power and frequency are not suitable for direct integration with UG [43]. Therefore, the FCBTBC with a developed control scheme is integrated as a link between the VSWT-PMSG and UG terminals. FCBTBC has three main control schemes: MPPT, MSC, and GSC as outlined in Figure 1. The MPPT algorithm calculates and generates the optimal rotating speed for the best wind energy harvesting. The MSC controller sets the rotor speed in accordance with the MPPT reference speed to attain maximum wind power [44] . Whilst the GSC controls the DC-link voltage, terminal voltage and current following the UG framework. The control schemes of the FCBTBC using the proposed SCA algorithm based -PI controller is elucidated in the following sections.

This article has been accepted for publication in a future issue of this journal, but has not been fully edited. Content may change prior to final publication. Citation information: DOI 10.1109/ACCESS.2021.3119019, IEEE Access

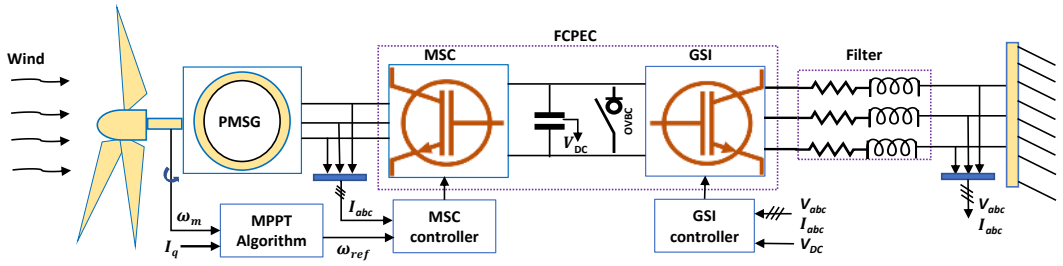

FIGURE 1: The configuration of grid-tied WECS

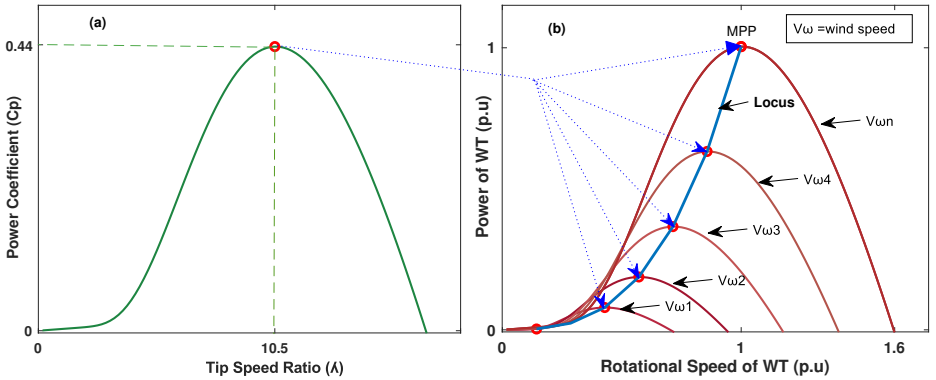

FIGURE 2: WT characteristics.(a) The Cp as a function of TSR. (b) The WT power as a function of rotational speed under various wind speeds

A. MPPT CONTROL SCHEME

In WECS, the output power of WT alters proportionally to the wind speed and the turbine rotational speed. For each wind turbine at any wind speed, there is only one optimal rotational speed ω_{m-opt}, that lead to a specified optimal TSR and maximizes captured wind power. As the wind speed changes continuously the WT is supposed to operate in a variable rotational speed mode in order to obtain the maximum wind power. To achieve this, it is required to incorporate an MPPT algorithm with a control scheme. The MPPT algorithm tracks the optimal rotational speed ω_{m-opt} at a given wind speed and provides the information to the MSC controller. Subsequently, the MSC controller drives the WT following the MPP trajectory [45]. In the conventional MPPT approach, the ω_{m-opt} of the WT rotor for each wind speed can be computed by Equation (10) [46].

$$\omega_{m-opt} = \frac{V_\omega \lambda_{opt}}{R} \tag{10}$$

Finding the optimal rotational speed ω_{m-opt} using this approach is simple although requires a precise wind speed measurement that is difficult to attain. The idea of tracking the optimal rotational speed without regard to wind speed is more reliable and promising. Therefore, in this work the optimal rotor speed could be estimated as:

$$\omega_{m-opt} = \sqrt[3]{\frac{P_m}{K_{opt}}} \tag{11}$$

where the value of K_{opt},and the generator power P_{m} are being obtained as:

$$\begin{cases} P_{\mathrm{m}} = \omega_m \left(J\frac{d\omega_m}{dt} + D\omega_m + \frac{3}{2}P_n\psi_f i_q \right) \\ K_{opt} = \frac{1}{2}\rho A C_{opt} \left(\frac{R}{\lambda_{\mathrm{opt}}} \right)^3 \end{cases} \tag{12}$$

The mechanical power P_m is calculated as a function of i_q and ω_m.

B. MSC CONTROL SCHEME

The main aim of the MSC is to maximise WT output power and attain the unity power factor at the PMSG terminal. At this end, an efficient cascaded control approach is needed to ensure optimal operation. Typically, the MSC has three controllers in its control scheme, and these are the speed controller (SCA-PI-1) and the two current controllers (SCA-PI-2 and SCA-PI-3) as illustrated in Figure 3. The SCA-PI-1 regulates the PMSG rotational speed to the optimal reference speed created by the MPPT algorithm. The SCA-PI-2 adjusts $q-$axis stator current ($I_{q.act}$) according to the set point ($I_{q.ref}$) given by SCA-PI-1 such that the maximum power is transferred to UG. Alternatively, the SCA-PI-3 is

applied to fix the d-axis stator current (I_d) to zero set point $(I_{d,ref})$ so as to attain unity power factor operation. The output signal of the SCA-PI-2 and SCA-PI-3 ($V_{d,ref}$ and $V_{q,ref}$) are converted to abc frame, $V_{abc,ref}$, by means of θ_r that is grasped from the PMSG speed. Subsequently, the $V^*_{a,b,c}$ signals are compared with a 1.65 kHz triangle carrier to produce IGBT switching signals for the MSC control scheme.

C. GSI CONTROL SCHEME

The connection of the VSWT-PMSG to the UG is achieved via a GSI. To ensure meeting the UG requirements, a cascaded vector scheme based SCA-PI for GSI is developed as shown in Figure 4. The GSI control scheme carries out two major tasks: first, controlling the DC-link capacitor voltage to its fixed point using the outer SCA-PI-4 controller, and secondly managing the quadrature and the direct currents (I_d and I_q) utilizing respective SCA-PI-5 and SCA-PI-6 based internal control loop. Here the Iq_{ref} is set to zero, so as to maintain the GSI operates at unity power factor. Afterwards, the output signal of the SCA-PI-6 $(V_{d,ref})$ and SCA-PI-6 $(V_{q,ref})$ are changed into three-phase frame signals $V^*_{a,b,c}$ by utilizing angle (θ_r). Angle (θ_r) that is retrieved from a phase-locked-loop (PLL) scheme. Finally, the carrier signal frequency is compared with the $V^*_{a,b,c}$ signals to generate firing pulses for the IGBT inverter.

D. DC-LINK PROTECTION SCHEME (DCLPS)

In case of a network disturbance, the GSI cannot injects the generated wind power into the UG due to the sudden voltage sag on the grid side. The voltage sag causes a sharp increase in DCL voltage and unbalanced power between the WECS and the grid side. The surplus energy may damage the inverter and the DCL capacitor. Owing to this, DCLPS is used to protect the system and keep the DCL voltage within permissible limits as depicted in Figure 1. In this study, a braking unit and relay are equipped with the DCL as a protection system. When the DCL voltage exceeds the allowed limit, the relay activates the braking unit. Furthermore, the braking unit prevents overvoltage of DCL by diverting through switching the excess energy to a resistor, which is then dissipated as heat.

IV. OPTIMIZATION MECHANISM

In this investigation, the SCA algorithm has to be coded in a MATLAB script file and linked with MATLAB/Simulink model for implementing online optimization of the PI controllers' gains. The developed Simulink model consists of twelve gains (proportional gain Kp and integral gain Ki) for the six PIs that exist in cascaded MSC and GSI control schemes as shown in Figures 3 and 4. The goal of the optimization procedure is to optimally design the PI controllers gains so as to enhance the performance of the grid-tied VSWT-PMSG. As the WECS is a highly non-linear dynamic system, it is difficult to determine its mathematical model or transfer function. That means it is not possible to develop a function that directly describes the relationship between the fitness function and the twelve PI controllers' gains. The alternative approach is by developing a controller design relationship based on an index of performance that takes into account the whole closed-loop response behavior. A performance evaluation index is a single measure of a system's performance that emphasis those characteristics of the response that are deemed to be important. A quite useful performance evaluation index is the integral square error (ISE) criterion. Therefore, in this work, the ISE criterion is used as a fitness function to formulate the optimization problem. The ISE can be modeled using the formula below:

$$ISE = \int_o^t \left(e^2_{\omega_m} + e^2_{iq_m} + e^2_{id_m} + e^2_{V_{dc}} + e^2_{iq_g} + e^2_{id_g}\right) dt \tag{13}$$

where e_{ω_m} denotes the error signals of the rotor speed. The e_{iq_m} and e_{id_m} are the i_q and i_d error signals of stator current respectively. The $e_{V_{dc}}$ represents the V_{dc} error signals, whereas e_{iq_g} and e_{id_g} signify the error signals of i_q grid and the i_d grid respectively. The optimization mechanism starts with initializing the proportional gains $(Kp1, Kp2, \ldots, Kp6)$ and integral gains $(Ki1, ki2, \ldots, Ki6)$ of all PIs which are regarded as the control variables of this optimization problem. The initial values of the PI's gains are generated randomly by the SCA, which are restricted to [0.5,15] so as to avoid divergence of the optimization process due to nonlinearities in the system. Then, all the PI controllers' error inputs are measured, squared, integrated, and then summed together. Following that, the sum of ISE is sent to the SCA algorithm as the objective function that has to be optimised. The main aim of the optimized problem is to reduce the ISE. At every single run of the grid-tied VSWT-PMSG Simulink model, the SCA assesses the ISE and generates new optimal gains for the PI controllers. This optimization procedure is iterated till the number of iterations condition is satisfied. The optimization mechanism flowchart for the SCA is described in Figure 5.

A. SCA ALGORITHM

SCA is a population-based optimization approach that is developed on the basis of sine and cosine arithmetic equations [33]. SCA, like other algorithms, begins the search process by generating a random set of solutions. Following this, the solutions are assessed using the objective function and enhanced by a set of rules toward the best ones. The algorithm then retains the solution which has been best reached as yet, identifies it as the destination, and updates solutions to generate new ones based on sine and cosine equations. Finally, the algorithm terminates the optimization process after the specified maximum number of iterations is reached. In terms of obtaining an ideal global solution, the SCA has been proven to be more efficient than other population-based algorithms [34]. The SCA algorithm updates the position of

This article has been accepted for publication in a future issue of this journal, but has not been fully edited. Content may change prior to final publication. Citation information: DOI 10.1109/ACCESS.2021.3119019, IEEE Access

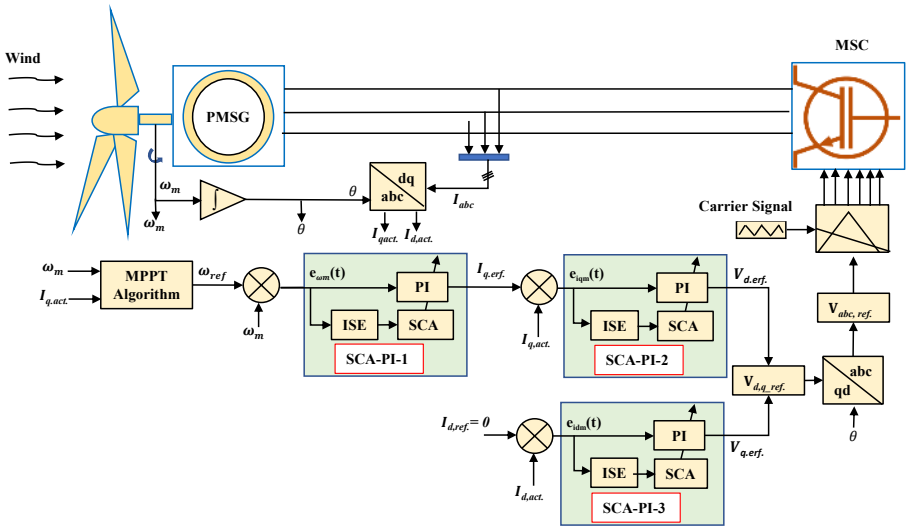

FIGURE 3: MSC control scheme

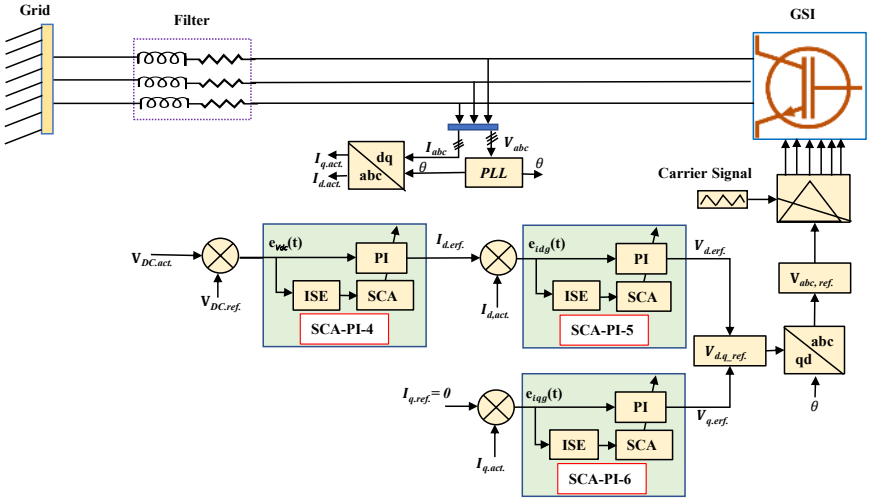

FIGURE 4: GSI control scheme

the solutions using Equations (14) and (15).

$$X_i^{t+1} = X_i^t + r_1 * Sin(r_2) * |r_3 P_i^t - X_i^t| \quad (14)$$

$$X_i^{t+1} = X_i^t + r_1 * Cos(r_2) * |r_3 P_i^t - X_i^t| \quad (15)$$

where X_i^t is the position of the current solution at the t^{th} iteration in the i^{th} dimension; P_i is the position of the destination point at the t^{th} iteration in the i^{th} dimension. Equations (14) and (15) are combined in equation (16).

$$X_i^{t+1} = \begin{cases} X_i^t + r_1 * Sin(r_2) * |r_3 P_i^t - X_i^t|, r_4 < 0.5 \\ X_i^t + r_1 * Cos(r_2) * |r_3 P_i^t - X_i^t|, r_4 \geq 0.5 \end{cases} \quad (16)$$

Equation (16) shows that SCA has four major parameters which are denoted as r_1, r_2, r_3, and r_4. The first parameter r_1 defines the movement direction (or next location regions), which may be within or outside the space between the destination and solution. The second parameter r_2 specifies the distance that the movement should be directed toward or away from the destination point. Parameter r_3 provides a random weight to the destination so as to emphasize ($r_3 > 1$) or de-emphasize ($r_3 < 1$) the influence of destination in defining the distance, stochastically. The parameter r_4 alternates the procedure between the cosine and sine parts. The random updated outside/inside position can be achieved by rearranging the sine-cosine mathematical functions as explained in [33]. Hence, this mechanism guarantees both diversification and intensification in the search space respectively. To maintain the balance between intensification and diversification, the sine and cosine Equations (14) and (15) are adapted and modified by applying Equation (17).

$$r_1 = a - t\frac{a}{T} \quad (17)$$

where T indicates the maximum iterations number and t is the currently running iteration. The a is a constant variable.

This article has been accepted for publication in a future issue of this journal, but has not been fully edited. Content may change prior to final publication. Citation information: DOI 10.1109/ACCESS.2021.3119019, IEEE Access

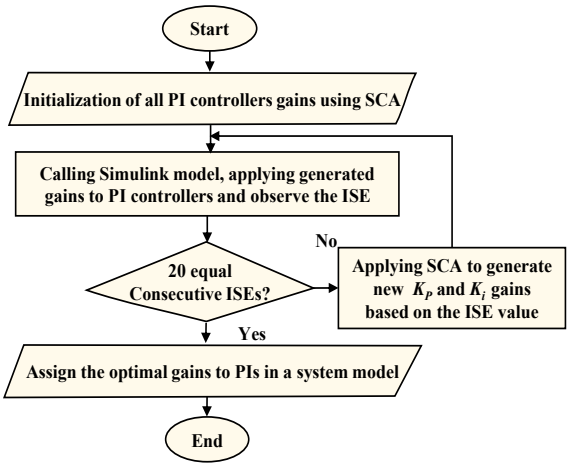

FIGURE 5: Flowchart of SCA optimization mechanism

The pseudo-code of the SCA algorithm is explained in algorithm 1.

Algorithm 1 SCA

Input:

- Set the lower bound and upper bound of X solutions between $0.5 \leq k_p$ and $k_i \leq 15$.
- Set the population size of N
- Randomly initialize the PIs Gains $\{kp_1,\ kp_2...kp_6\}$ & $\{ki_1,\ ki_2...ki_6\}$
- Specify Max iterations T

Output:

- The best-selected solution (X^*) for PIs gain values

Loop Process

while $(t \leq Max\ iterations\ T)$ **do**
  Calculate fitness function (ISE)
  Define the best-selected solution (X^*)
  Update r_1, r_2, r_3, and r_4
  Update agents' locations in the search space with (16)
end while
Return (X^*) **for PIs Gain values**
Save best obtained PIs gain values

B. GWO ALGORITHM

Grey Wolf Optimizer (GWO) is a meta-heuristic algorithm that is inspired by a social hierarchy of grey wolves and their mechanism for hunting [47]. The GWO algorithm's leadership hierarchy is described as alpha (α), beta (β), delta (δ), and omega (ω) levels. The alpha is considered the wolves leader, who is responsible for deciding on the hunting, the sleeping place, get-up time, and so on. It is also referred to as the dominant wolf, as his/her commands must be obeyed by the pack. Beta wolf is the second level in the grey wolf hierarchy, and its function is to assist alpha in making decisions. The next subordinate to alpha and beta is delta which helps in controlling the majority of wolves in the hierarchical population. The omega wolves must be subjected to the wolves in the first three levels in order to maintain the hierarchical structure's safety. The hunting strategy of grey wolves involves tracking, encircling, harassing, and finally attacking the prey. This behaviour can be mathematically formulated as follows:

$$\vec{D} = \left| \vec{C} \cdot \overrightarrow{X_p}(t) - \vec{X}(t) \right| \tag{18}$$

$$\vec{X}(t+1) = \overrightarrow{X_p}(t) - \vec{A} \cdot \vec{D} \tag{19}$$

$\overrightarrow{X_p}$ represents the prey position vector, t denotes the current iteration, $\vec{A}$ and $\vec{C}$ express coefficient vectors, and $\vec{X}$ signifies a gray wolf location vector. The vectors $\vec{C}$ and $\vec{A}$ are computed using Equation (20).

$$\begin{aligned} \vec{A} &= 2\vec{a} \cdot \overrightarrow{r_1} - \vec{a} \\ \vec{C} &= 2 \cdot \overrightarrow{r_2} \end{aligned} \tag{20}$$

where r_1 and r_2 are random vectors in [0, 1], and components of a are linearly lowered from 2 to 0 during the course of iterations. Prey hunting is often performed by α and β with δ participating on occasion. The leaders α begin assaulting the prey, supported by the secondary leaders β and the followers δ. The equation (21) (22) and (23) describe this behaviour.

$$\begin{aligned} \overrightarrow{D_\alpha} &= \left| \overrightarrow{C_1} \cdot \overrightarrow{X_\alpha} - \vec{X} \right|, \\ \overrightarrow{D_\beta} &= \left| \overrightarrow{C_2} \cdot \overrightarrow{X_\beta} - \vec{X} \right|, \\ \overrightarrow{D_\delta} &= \left| \overrightarrow{C_3} \cdot \overrightarrow{X_\delta} - \vec{X} \right|, \end{aligned} \tag{21}$$

$$\begin{aligned} \overrightarrow{X_1} &= \overrightarrow{X_\alpha} - \overrightarrow{A_1} \cdot \left(\overrightarrow{D_\alpha} \right) \\ \overrightarrow{X_2} &= \overrightarrow{X_\beta} - \overrightarrow{A_2} \cdot \left(\overrightarrow{D_\beta} \right), \\ \overrightarrow{X_3} &= \overrightarrow{X_\delta} - \overrightarrow{A_3} \cdot \left(\overrightarrow{D_\delta} \right) \end{aligned} \tag{22}$$

$$\vec{X}(t+1) = \frac{\overrightarrow{X_1}(t) + \overrightarrow{X_2}(t) + \overrightarrow{X_3}(t)}{3} \tag{23}$$

Algorithm 2 outlines the pseudo-code of the GWO algorithm.

C. PSO ALGORITHM

The PSO algorithm is a swarm intelligence search method that mimics the social behavior of birds in a flock [48], [49]. It is built on individual knowledge connection and natural learning during birds seek food and migrating in the search area. The PSO algorithm begins the search with a randomly generated particle P population, each representing a possible solution. Each particle contains two vectors: a position vector (d) and a velocity vector (v). The velocity and position of every single particle are altered using update equations which take into account the history of the best individual P_{best} and best entire experiences solutions G_{best}. The particle's updated velocity and position are represented in Equations (24) and (25) respectively :

$$v_{i+1}^k = \omega_i v_i^k + c_1 r_1 \left(P_{best,i}^k - d_i^k \right) + c_2 r_2 \left(G_{best,i} - d_i^k \right) \tag{24}$$

Algorithm 2 GWO

Input:

- Set the boundary of initial values for search agents $\vec{X}(t) = \{k_{p1}, k_{p2}, \ldots, k_{p6}, k_{i1}, k_{i2} \ldots, k_{i6}\}$ between $0.5 \leq k_p$ and $k_i \leq 15$.
- Initialize parameters a, A and C.
- Specify the max iterations T.

Output:

- Evaluate the fitness function ISE $\vec{X}(t)$.

loop Process

while $(t \leq T)$ **do**
  Modify a, A, and C
  Update the search agents $\vec{X}(t+1)$ by Equation(23)
  Compare ISE $\vec{X}(t)$ with ISE $\vec{X}(t+1)$
  Update $\overrightarrow{X_\alpha}$ $\overrightarrow{X_\beta}$ and $\overrightarrow{X_\delta}$
  $t = t + 1$
end while
Send the best solution $\overrightarrow{X_\alpha}$.

$$d_{i+1}^k = d_i^k + v_{i+1}^k \tag{25}$$

where, c_1 and c_2 signify the speedup coefficients. k is the number of swarms. Whereas r_1 and r_2 are random values in the range of $[0, 1]$. The ω depicts the weight of inertia. Moreover, $P_{\text{best},i}$ is the individual best solution of particle i, and $G_{\text{best},i}$ is the global best of $P_{\text{best},i}$ based on the entire population experiences. More details of the PSO algorithm used to design the gains of the PI controllers are given in [50].

D. OPTIMIZATION RESULTS AND STATISTIC ANALYSIS

1) Optimization Results

It is worth mentioning that all algorithms are utilised for online optimization. Therefore, during the optimization procedure, the SCA, GWO, and PSO algorithms are directly performed to reduce the fitness function (ie., the ISE) so as to obtain the optimal PIs gains. These algorithms are coded in MATLAB scripts and linked to MATLAB Simulink. The iterations number is decided by the algorithm itself based on 20 equal consecutive ISE of $5^{-}8$ tolerance. The simulation time for each iteration is set to 30 seconds. The gain values of the optimized PI controllers utilizing the SCA, GWO, and PSO algorithms are listed in Table 1. The optimal PI controller gains obtained by the SCA algorithm are the best as it grants the lowest fitness function.

2) Statistical Analysis

To validate reliability of the optimization results, statistical analysis of execution time, convergence time, and iteration number for all the algorithms are performed, as provided in the Table 3. The static finding confidently verify that the SCA outperforms the GWO and PSO algorithms in terms of the lowest mean iteration number, the shortest mean execution time, and the shortest mean convergence times (highlighted in bold) due to its effectiveness. Figure 6 shows the convergence speed and terminating iterations of the three algorithms.The Figure 6 reveals that ISE minimization utilising SCA has a faster convergence speed than GWO and PSO. Consequently, its optimization iteration was terminated first as the tolerance condition has been reached early. In this context, convergence refers to the first an algorithm finds a minimal fitness function in the intended iterations. Table 2 manifests the statistical outcomes of the fitness function gained by SCA, GWO and PSO algorithms in ten runs. The findings confirmed that the SCA algorithm has the lowest performance indices out of the other algorithms that have been tested. consider that the smallest mean value shows that SCA is able to find a better value with a smaller fitness function, while, the lowest standard deviation and the lowest variance indicate that convergence stability, reliability, and identicality are at the highest levels.

3) Significance Analysis

For further verification, the one-way analysis of variance (ANOVA) test was employed to determine whether the differences between the resulting ISE generated by the proposed algorithm and other algorithms were statistically significant. The null hypothesis assumes no significant difference in ISE between the proposed algorithm and other existing algorithm. At a state level larger than 0.05, the null hypothesis is accepted, while at a state level less than 0.05, it is rejected. Since this work aims to find the significant differences for more than two algorithms, the ANOVA test technique is selected for this purpose. The obtained P-value of 0.0047 shown in Table 4 indicates that the null hypothesis is rejected and also conforms that there is a significant difference between the proposed SCA algorithm and the others algorithms. Beside, Figure 7 shows the boxplot of the significant differences between the proposed algorithm and others.

TABLE 1: Optimal gains of PI controllers

Algorithm	PIs	K_p	K_i
SCA	PI-1	8.0691	12.1318
	PI-2	8.5465	15.0000
	PI-3	0.6952	9.7200
	PI-4	1.1397	1.2810
	PI-5	0.7269	0.5000
	PI-6	4.5862	2.5109
GWO	PI-1	12.2386	15
	PI-2	5.88106	14.8518
	PI-3	0.5	12.8013
	PI-4	0.5	0.648046
	PI-5	0.793491	3.23962
	PI-6	5.09131	1.10481
PSO	PI-1	1.31914	11.3975
	PI-2	7.41449	7.11482
	PI-3	1.62522	14.2915
	PI-4	3.74789	0.610424
	PI-5	0.918551	1.41182
	PI-6	1.76885	6.53668

This article has been accepted for publication in a future issue of this journal, but has not been fully edited. Content may change prior to final publication. Citation information: DOI 10.1109/ACCESS.2021.3119019, IEEE Access

TABLE 2: Statistical results of fitness function obtained by different algorithms in 10 runs.

Algorithm	Best	Worst	Mean	Standard Deviation	Variance
SCA	**0.18059**	**0.24624**	**0.20228**	**0.01949**	**0.00038**
GWO	0.19192	0.34229	0.23654	0.04851	0.00235
PSO	0.22384	0.36586	0.26797	0.04665	0.00218

TABLE 3: The statistical results of execution convergence time and iteration number obtained by different algorithms

Algorithm	Execution time(h)			Convergence time(h)			Iteration numbers		
	Max.	Min.	Mean	Max.	Min.	Mean	Max.	Min.	Mean
SCA	**2.52845**	**1.75815**	**2.17891**	**1.86000**	**0.94040**	**1.42912**	**61**	**43**	**52**
GWO	3.14831	2.32120	2.75352	2.33057	1.49220	1.93136	77	56	67
PSO	3.59057	2.54490	2.96870	2.75555	1.76185	2.13208	86	61	71

TABLE 4: ANOVA table results on ISE

Source	SS	df	MS	F	*P*-Value
Groups	0.02159	2	0.01079	6.6	**0.0047**
Error	0.04419	27	0.00164		
Total	0.06578	29			

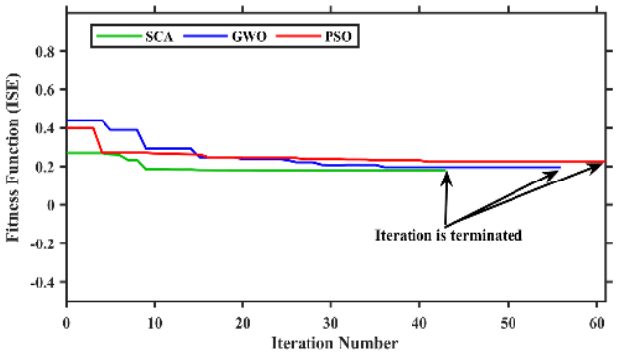

FIGURE 6: Algorithms Fitness function convergence

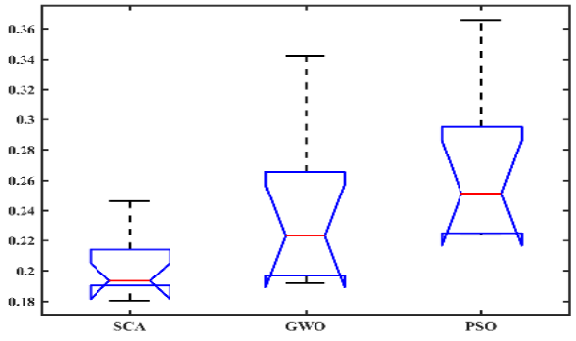

FIGURE 7: Boxplot differences of results on ISE.

V. SIMULATION ANALYSIS AND DISCUSSION

The WECS shown in Figure 1 is implemented and simulated in the MATLAB/Simpower environment. The main objective of the simulation is to assess the effectiveness and accuracy of the proposed SCA-PI control schemes for the grid-connected VSWT-PMSG. To ascertain the robustness of the SCA-PI control scheme the system have been tested under dynamic and transient circumstances. Besides, the simulation results of the SCA-PI control scheme are compared to those of the GWO-PI and PSO-PI control schemes, and it can be verified that SCA-PI is the better algorithm. The simulation times are configured to 10, and 100 seconds for transient and dynamic conditions respectively. The simulation parameters settings of the WECS are tabled in Appendix A.

A. TRANSIENT CIRCUMSTANCE EVALUATION

This part analyzes the system's behaviour during a network disturbance due to a fault which might happen any point in the grid that can leads to voltage drop at the Point of common coupling (PCC). The analysis seeks to appraise the effectiveness of the SCA-PI control scheme at improving VSWT- PMSG's transient stability response. In the simulation, it is assumed that a three-phase fault in the utility grid occurred at t = 3 seconds. The wind speed is assumed to remain constant at 12 m/s as the duration of the transient circumstance is very short. During the fault occurrences, the over current relay detected the surpassed current and triggered the circuit breaker to open. Consequently, the fault has been successfully eliminated according to the relay time delay of 0.4 seconds.

During a network disturbance, the voltage at PCC can descends suddenly from its rated value of 1.0 up to less than 0.5 p.u. The GSI controller compensates the voltage dip by injecting reactive power into the system as an extra ancillary services to assist network stability. As a result, the grid voltage recovered to the pre-fault value of 1 p.u as depicted in Figure 8 (a). The response of SCA-PI scheme for transient circumstance has been compared with the PSO-PI and GWO-PI schemes. The results confirmed that PCC voltage response using the SCA-PI approach was better damped with lower peak undershoot (PUsh) as compared to that realized when using GWO-PI or PSO-PI approaches. On the other hand, when the PCC voltage dropped, the DC link voltage (V_{DCL}) is increased due to the grid's active power reduction, while the generated active power from the PMSG remains constant. The V_{DCL} raises rapidly at the moment of failure, leading to unstable operation of the FCBTC. In order to keep the V_{DCL} response within an acceptable range

This article has been accepted for publication in a future issue of this journal, but has not been fully edited. Content may change prior to final publication. Citation information: DOI 10.1109/ACCESS.2021.3119019, IEEE Access

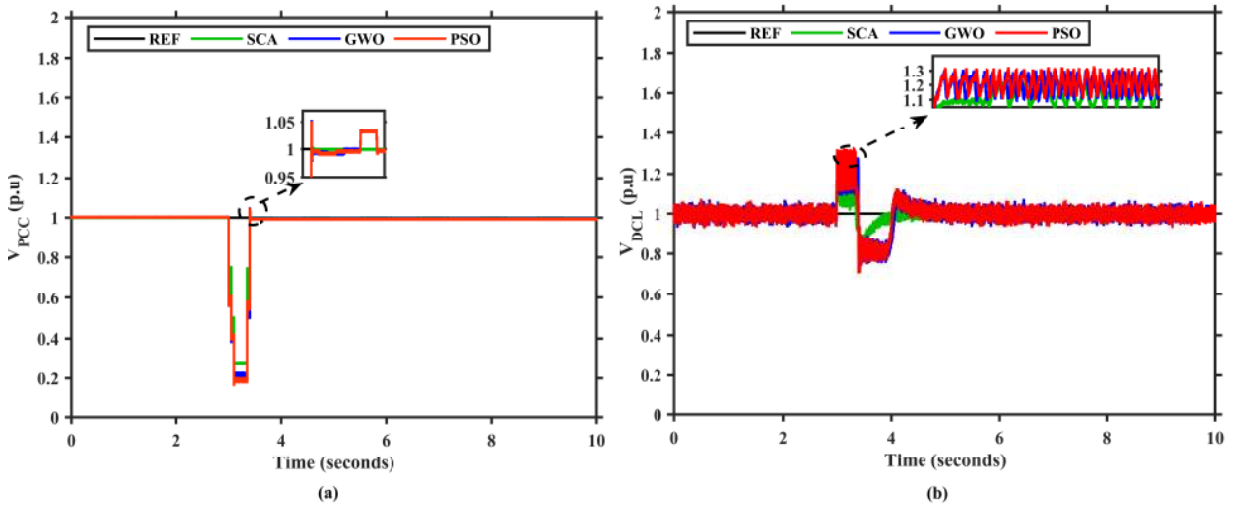

FIGURE 8: System response under transient circumstance.(a) V_{PPC}. (b) V_{DCL}

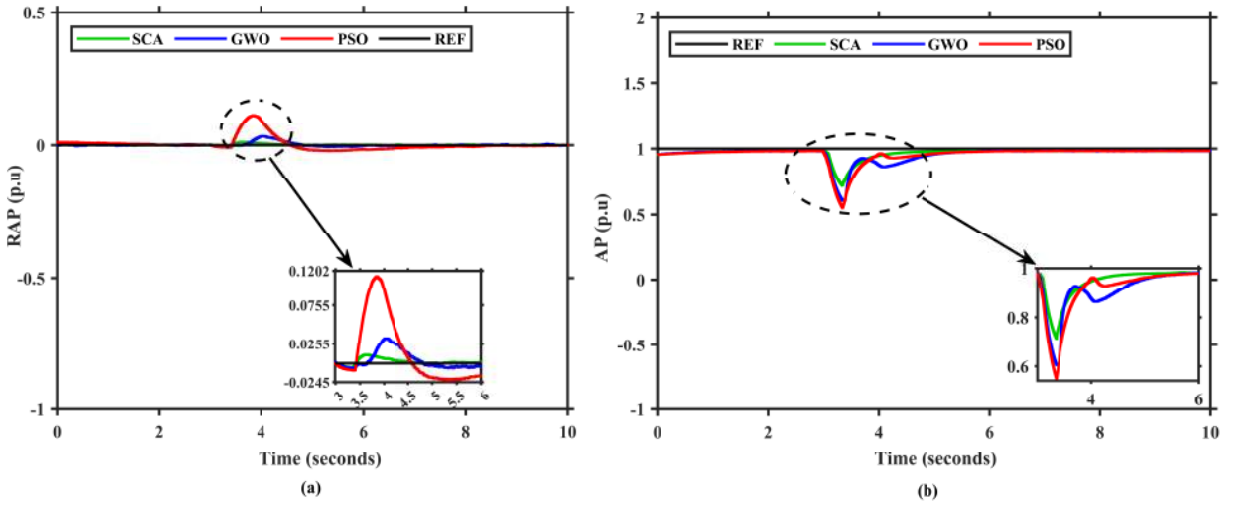

FIGURE 9: System response under transient circumstance (a) RAP (b) AP

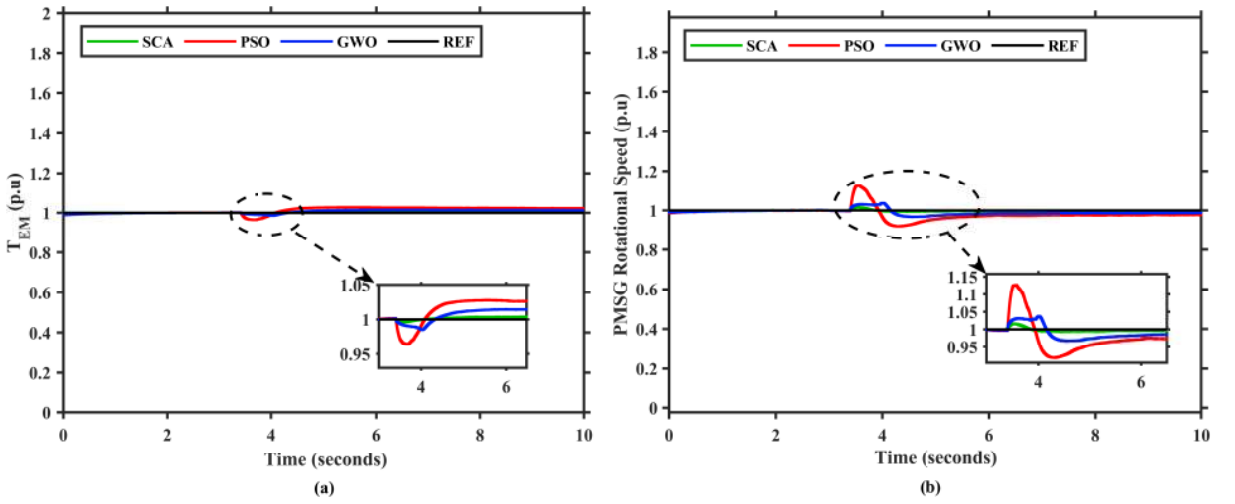

FIGURE 10: System response under transient circumstance (a) T_{EM}. (b) PMSG Speed

during a fault situation, the DCLPS with a brake unit and relay was considered in this proposed control scheme. Figure 8 (b) showed that the proposed SCA-PI approach achieved a much faster reaction, lower peak overshoot (POsh) and less alteration in the DC-link voltage than the GWO-PI as well as the PSO- PI approaches.

The performance of the Active power (AP) and Reactive power (RAP) at PCC are illustrated in Figure 9. The active power deteriorates and reactive power increases to recover the system into healthy condition. The outcome demonstrated that the reactive power compensation for voltage recovery support using the SCA-PI gives the lowest value and the most enhanced as compared to the GWO-PI as well as the PSO-PI as manifested in Figure 9 (a) . In addition, as demonstrated in Figure 9 (b), the deterioration in active power gives the lowest value when the SCA-PI control scheme is used. The SCA-PI control scheme is able to transmit maximum AP to the UG with a faster settling time (Ts), lower PUsh and less SSE as compared to the GWO-PI as well as the PSO-PI control schemes. Moreover, the result shown in Figure 10 (a) confirmed the SCA-PI surpassed the GWO-PI and PSO-PI in controlling the electromagnetic torque (T_{EM}) via the q-axis stator current. Hence, the generator rotational speed return to its rated value reasonably fast with POsh of less than 2 % despite of the transient event as illustrate in Figure (b) 10. Table 5 provides details of the system's transient behavior, including the SSE, the POsh percentage, the PUsh percentage, and the Ts for the three algorithms. The settling time has been measured with respect to starting network disturbance. According to the results of the transient behaviour, the SCA-PI control scheme can be considered a precise method of enhancing the transient performance of VSWT-PMSG.

TABLE 5: Details of transient behaviour

System response	Specification	SCA-PI	GWO-PI	PSO-PI
V_{PCC}	SSE (pu)	0.0004	0.004	0.007
	PUsh (%)	73	78	84
	Ts (s)	0.4	0.41	0.41
V_{DCL}	POsh (%)	20	31.6	32
	Ts (s)	0.93	1.19	1.5
RAP_{pcc}	SSE (pu)	0.004	0.022	0.013
	POsh (%)	1.37	12.5	3.69
	Ts (s)	0.4	1.4	2.6
AP_{pcc}	SSE (pu)	0.017	0.0188	0.019
	PUsh (%)	26.35	37.63	43.04
	Ts (s)	1.12	2.02	1.61
PMSG Speed	SSE (pu)	0.004	0.012	0.022
	POsh (%)	1.6	4.9	14.8
	Ts (s)	0.4	1.67	2.07
T_{EM}	SSE (pu)	0.004	0.014	0.023
	PUsh (%)	0.9	2.8	6
	Ts (s)	0.4	1.13	1.08

B. DYNAMIC CIRCUMSTANCE EVALUATION

The wind speed fluctuations is a major challenge that faces the control schemes of WECS. To test the robustness and performance of the proposed SCA-PI scheme during sudden and erratic changes in wind speed, a stochastic wind speed profile represented in Figure 11(a) is applied. It is randomly changed between 8 m/s and 12 m/s for a duration of 100 seconds to mimic a more realistic wind speed in reality. The performance of the proposed SCA-PI has been also compared to the performance of GWO-PI as well as PSO-PI under the same circumstances. The results shown in Figure 11 (b) confirmed that the SCA-PI is capable of regulating the PMSG rotational speed according to wind speed changes with its optimal value better than GWO-PI as well as PSO-PI. Moreover, the proposed SCA-PI scheme outperformed the GWO-PI and PSO-PI schemes in tracking the optimal Cp (0.44) and TSR (10.5) values , as shown in Figure 12 (a, b) respectively. This, in turn, possesses a direct impact on the maximum power extraction from available wind energy.

To further show the performance of the proposed SCA-PI under variation of wind speed conditions, the APpcc and RAPpcc have been analysed. The simulation results for APpcc and RAPpcc under the assessed wind speed profile in all control schemes are shown in Figure.13 (a, b) respectively.Figure 13 (a) confirms that when SCA-PI is used, the injected active power into UG is more precise and closer to the rated value than when applying GWO-PI or PSO-PI. It is observed that the active power injected into the utility grid is extremely close to the maximum power due to power losses of the power converter. Besides, Figure 13 (b) also confirms that the SCA-PI control scheme has more capability and robustness than the PI GWO-PI and the PSO-PI in terms of adjusting the RAP to zero with a lower Osh. In Figure 14 (a), it is clearly shown that the SCA-PI controls the Vpcc with small SSE and has low oscillations around the reference voltage as compared to the GWO-PI and the PSO-PI control schemes. The notable performance of the proposed SCA-PI scheme is visible in the magnified views in Figure 14 (a), where the SSE of SCA-PI GWO-PI and PSO-PI are 0.001 p.u , 0.006 p.u and 0.011p.u respectively. To complete the analysis evaluation, Figure 14 (b) depicts the V_{DCL} performance. The very good regulation achieved for theV_{DCL} when using the SCA-PI as compared to GWO-PI and PSO-PI can be recognized. Hence, it can be deduced that the proposed SCA-PI shows a noticeable performance and robustness as compared to GWO-PI and PSO-PI. Likewise, it can be observed that the GWO-PI control approach is better than the PSO-PI approach.

In general, the simulation findings have fully revealed the superior advantage of the proposed SCA-PI in the controlling of the predefined parameters under variation of wind speed profile. The proposed SCA-PI showed its capability in keeping Cp, TSR at optimal values with fewer deviations and penetrating the maximum power into UG. In addition, the SCA-PI possesses the capability of regulating Vpcc, V_{DCL}, RAPpcc at rated value regardless of the wind speed fluctuations. Last but not least, when the simulation results of the three approaches are compared, it can be inferred that SCA-PI approach has more capability in reducing the system's POsh, PUsh, SSE and oscillation better than the

This article has been accepted for publication in a future issue of this journal, but has not been fully edited. Content may change prior to final publication. Citation information: DOI 10.1109/ACCESS.2021.3119019, IEEE Access

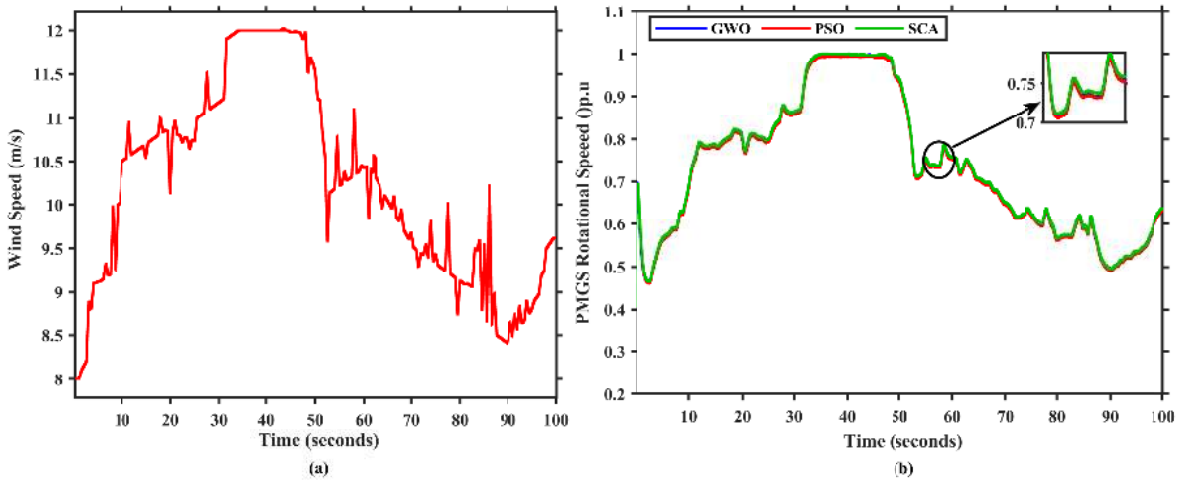

FIGURE 11: System response under dynamic circumstance (a) Wind speed Profile . (b) PMSG Rotational Speed

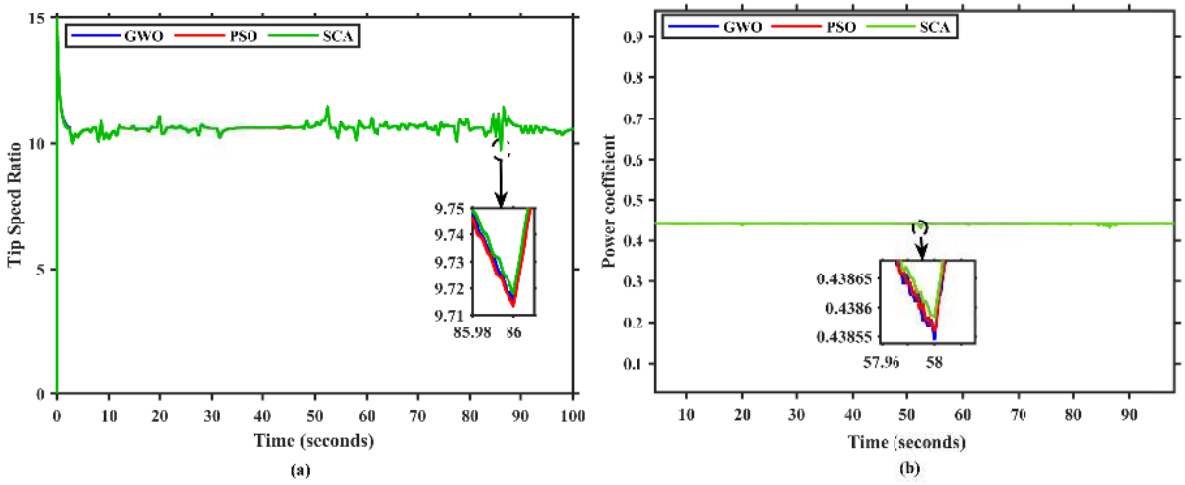

FIGURE 12: System response under dynamic circumstance (a)Tip Speed Ratio . (b) Power Coefficient

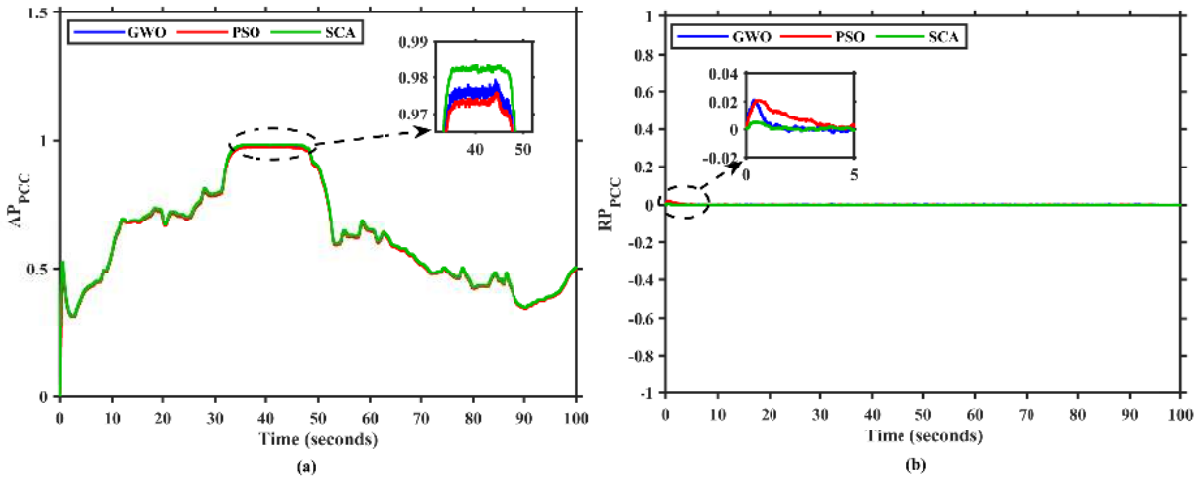

FIGURE 13: System response under dynamic circumstance (a) AP at PCC (b) RAP at PCC

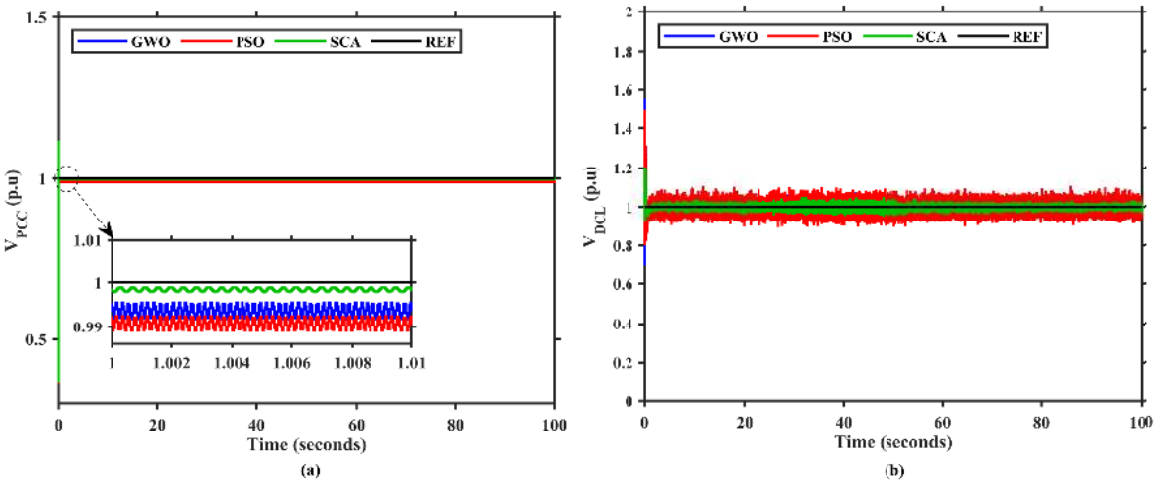

FIGURE 14: System response under dynamic circumstance (a) V_{pcc} (b) V_{DCL}

other two approaches.

VI. CONCLUSION

This work has presented a unique implementation of the SCA algorithm to optimize the gains of cascaded PI controllers when integrated in BTBC control schemes of the grid-tied VSWT-PMSG. The optimization procedure aims to get the best possible values for PI gains that lead to extraction of the maximum wind power and enhance the WECS performance under dynamic and transient operating conditions. With regards to this, the SCA picks the optimal PI controllers gains based on the minimum ISE summation of system variables. The performance of the proposed SCA-PI control scheme has been evaluated under grid fault and fluctuating wind speed circumstances. Moreover, SCA-PI performance has also been compared with GWO-PI and PSO-PI performances under the same operating conditions. Simulation findings confirmed that the SCA-PI control scheme outperforms the GWO-PI and PSO-PI control schemes in terms of PUsh, POsh, SSE, Ts and damping system oscillations under the dynamic and transient operations conditions. The notable performance of the proposed control scheme is due to the good design of the SCA during the design process, which relies on the designer's knowledge.

The contribution of this paper shall draw promising future research directions from the fact that where in by integrating the SCA algorithm with a control scheme has proven to be a significant influence on the performance of the grid-connected wind energy convergence system. The SCA algorithm has produced satisfactory results with regards to its current features and can be extended to develop a hybrid of the SCA algorithm with another algorithm and then validate against the state-of-the-art meta-heuristic optimization algorithms to assess viability of the hybrid algorithm.

ACKNOWLEDGMENT

The authors acknowledge the support from Ministry of Higher Education Malaysia and Universiti Teknologi PETRONAS for the award of Fundamental Research Grant scheme (FRGS/1/2019/TK04/UTP/02/10) and Graduate research assistantship scheme.

.

APPENDIX A PARAMETERS WECS

TABLE 6: Parameters of WECS

Parameter	Symbol	Value
Rated power	P	$1.5MW$
Air density	ρ	$1.225\ kg/m^3$
Rated wind speed	V_ω	$12\ m/s$
Blade radius	R	$33.5\ m$
Optimal TSR	λ_{opt}	10.5
Opt. Power Coefficient	$C_{p.opt}$	0.44
Inertia	J	$0.032\ kgm^2$
Number of poles pair	P_n	48
Stator resistance	R_s	$0.135\ \Omega$
Stator inductance(d-axis)	L_{ds}	$4\ mH$
Stator inductance(q-axis)	L_{qs}	$4\ mH$
Magnetic flux	ψ_f	$0.5V.S$
Frequency	F	$50\ Hz$
DC link capacitance	C	$650\ \mu F$
Dc-link voltage	V_{DCL}	$1.15\ kV$
Grid voltage	Vg	$575V$

REFERENCES

[1] M.-A. Akbari, J. Aghaei, and M. Barani, "Convex probabilistic allocation of wind generation in smart distribution networks," IET Renewable Power Generation, vol. 11, no. 9, pp. 1211–1218, 2017.

[2] Global Wind Energy Council, "Global wind report 2021," Accessed July. 11, 2021. [Online]. Available: https://gwec.net/global-wind-report-2021/

[3] statista, "Projected global cumulative wind power capacity from 2017 to 2022"," Accessed June. 21, 2021. [Online]. Available: https://www.statista.com/statistics/185551/global-wind-market-forecast-by-cumulative-capacity-since-2010/

[4] B. K. Sahu, "Wind energy developments and policies in china: A short review," Renewable and Sustainable energy reviews, vol. 81, pp. 1393–1405, 2018.

[5] E. Joshua and R. Sthuthi, Wind power technology, 3rd ed. PHI Learning Pvt. Ltd., 2019.

[6] X. Zeng, T. Liu, S. Wang, Y. Dong, and Z. Chen, "Comprehensive coordinated control strategy of pmsg-based wind turbine for providing frequency regulation services," IEEE Access, vol. 7, pp. 63 944–63 953, 2019.

[7] M. Zribi, M. Alrifai, and M. Rayan, "Sliding mode control of a variable-speed wind energy conversion system using a squirrel cage induction generator," Energies, vol. 10, no. 5, p. 604, 2017.

[8] S. Karad and R. Thakur, "Recent trends of control strategies for doubly fed induction generator based wind turbine systems: A comparative review," Archives of Computational Methods in Engineering, vol. 28, no. 1, pp. 15–29, 2021.

[9] R. Basak, G. Bhuvaneswari, and R. R. Pillai, "Low-voltage ride-through of a synchronous generator-based variable speed grid-interfaced wind energy conversion system," IEEE Transactions on Industry Applications, vol. 56, no. 1, pp. 752–762, 2019.

[10] D. Reddy and S. Ramasamy, "Design of rbfn controller based boost type vienna rectifier for grid-tied wind energy conversion system," IEEE Access, vol. 6, pp. 3167–3175, 2018.

[11] S. Tripathi, A. Tiwari, and D. Singh, "Grid-integrated permanent magnet synchronous generator based wind energy conversion systems: A technology review," Renewable and Sustainable Energy Reviews, vol. 51, pp. 1288–1305, 2015.

[12] V. Yaramasu, A. Dekka, M. J. Durán, S. Kouro, and B. Wu, "Pmsg-based wind energy conversion systems: survey on power converters and controls," IET Electric Power Applications, vol. 11, no. 6, pp. 956–968, 2017.

[13] N. D. Dao, D.-C. Lee, and S. Lee, "A simple and robust sensorless control based on stator current vector for pmsg wind power systems," IEEE Access, vol. 7, pp. 8070–8080, 2018.

[14] S. M. Mozayan, M. Saad, H. Vahedi, H. Fortin-Blanchette, and M. Soltani, "Sliding mode control of pmsg wind turbine based on enhanced exponential reaching law," IEEE Transactions on Industrial Electronics, vol. 63, no. 10, pp. 6148–6159, 2016.

[15] R. Tiwari, S. Padmanaban, and R. B. Neelakandan, "Coordinated control strategies for a permanent magnet synchronous generator based wind energy conversion system," Energies, vol. 10, no. 10, p. 1493, 2017.

[16] M. A. Soliman, H. M. Hasanien, H. Z. Azazi, E. E. El-Kholy, and S. A. Mahmoud, "An adaptive fuzzy logic control strategy for performance enhancement of a grid-connected pmsg-based wind turbine," IEEE Transactions on Industrial Informatics, vol. 15, no. 6, pp. 3163–3173, 2018.

[17] R. Errouissi, A. Al-Durra, and M. Debouza, "A novel design of pi current controller for pmsg-based wind turbine considering transient performance specifications and control saturation," IEEE Transactions on Industrial Electronics, vol. 65, no. 11, pp. 8624–8634, 2018.

[18] S. M. Tripathi, A. N. Tiwari, and D. Singh, "Controller design for a variable-speed direct-drive permanent magnet synchronous generator-based grid-interfaced wind energy conversion system using d-partition technique," IEEE Access, vol. 5, pp. 27 297–27 310, 2017.

[19] W. Cao, N. Xing, Y. Wen, X. Chen, and D. Wang, "New adaptive control strategy for a wind turbine permanent magnet synchronous generator (pmsg)," Inventions, vol. 6, no. 1, p. 3, 2021.

[20] M. A. Soliman, H. M. Hasanien, A. Al-Durra, and I. Alsaidan, "A novel adaptive control method for performance enhancement of grid-connected variable-speed wind generators," IEEE Access, vol. 8, pp. 82 617–82 629, 2020.

[21] M. I. Mosaad, H. S. M. Ramadan, M. Aljohani, M. F. El-Naggar, and S. S. Ghoneim, "Near-optimal pi controllers of statcom for efficient hybrid renewable power system," IEEE Access, vol. 9, pp. 34 119–34 130, 2021.

[22] H. M. Hasanien, "Gravitational search algorithm-based optimal control of archimedes wave swing-based wave energy conversion system supplying a dc microgrid under uncertain dynamics," IET Renewable Power Generation, vol. 11, no. 6, pp. 763–770, 2017.

[23] M. H. Qais, H. M. Hasanien, and S. Alghuwainem, "Augmented grey wolf optimizer for grid-connected pmsg-based wind energy conversion systems," Applied Soft Computing, vol. 69, pp. 504–515, 2018.

[24] M. M. Hato, S. Bouallègue, and M. Ayadi, "Water cycle algorithm-tuned pi control of a doubly fed induction generator for wind energy conversion," in 2018 9th international renewable energy congress (IREC). IEEE, 2018, pp. 1–6.

[25] B. Yang, T. Yu, H. Shu, X. Zhang, K. Qu, and L. Jiang, "Democratic joint operations algorithm for optimal power extraction of pmsg based wind energy conversion system," Energy Conversion and Management, vol. 159, pp. 312–326, 2018.

[26] M. H. Qais, H. M. Hasanien, and S. Alghuwainem, "A grey wolf optimizer for optimum parameters of multiple pi controllers of a grid-connected pmsg driven by variable speed wind turbine," IEEE Access, vol. 6, pp. 44 120–44 128, 2018.

[27] A.-A. A. Mohamed, A. L. Haridy, and A. Hemeida, "The whale optimization algorithm based controller for pmsg wind energy generation system," in 2019 international conference on innovative trends in computer engineering (ITCE). IEEE, 2019, pp. 438–443.

[28] Y.-S. Kim, I.-Y. Chung, and S.-I. Moon, "Tuning of the pi controller parameters of a pmsg wind turbine to improve control performance under various wind speeds," Energies, vol. 8, no. 2, pp. 1406–1425, 2015.

[29] M. H. Qais, H. M. Hasanien, and S. Alghuwainem, "Optimal transient search algorithm-based pi controllers for enhancing low voltage ride-through ability of grid-linked pmsg-based wind turbine," Electronics, vol. 9, no. 11, p. 1807, 2020.

[30] N. H. Saad, A. A. El-Sattar, and M. E. Marei, "Improved bacterial foraging optimization for grid connected wind energy conversion system based pmsg with matrix converter," Ain Shams Engineering Journal, vol. 9, no. 4, pp. 2183–2193, 2018.

[31] M. A. Soliman, H. M. Hasanien, S. Alghuwainem, and A. Al-Durra, "Symbiotic organisms search algorithm-based optimal control strategy for efficient operation of variable-speed wind generators," IET renewable power generation, vol. 13, no. 14, pp. 2684–2692, 2019.

[32] M. H. Qais, H. M. Hasanien, and S. Alghuwainem, "A novel lmsre-based adaptive pi control scheme for grid-integrated pmsg-based variable-speed wind turbine," International Journal of Electrical Power & Energy Systems, vol. 125, p. 106505, 2021.

[33] S. Mirjalili, "Sca: a sine cosine algorithm for solving optimization problems," Knowledge-based systems, vol. 96, pp. 120–133, 2016.

[34] A. Alqushaibi, S. J. Abdulkadir, H. M. Rais, Q. Al-Tashi, M. G. Ragab, and H. Alhussian, "Enhanced weight-optimized recurrent neural networks based on sine cosine algorithm for wave height prediction," Journal of Marine Science and Engineering, vol. 9, no. 5, p. 524, 2021.

[35] A. Daoui, H. Karmouni, M. Sayyouri, H. Qjidaa, M. Maaroufi, and B. Alami, "New robust method for image copyright protection using histogram features and sine cosine algorithm," Expert Systems with Applications, vol. 177, p. 114978, 2021.

[36] A.-F. Attia, R. A. El Sehiemy, and H. M. Hasanien, "Optimal power flow solution in power systems using a novel sine-cosine algorithm," International Journal of Electrical Power & Energy Systems, vol. 99, pp. 331–343, 2018.

[37] S. Gupta, K. Deep, and A. P. Engelbrecht, "A memory guided sine cosine algorithm for global optimization," Engineering Applications of Artificial Intelligence, vol. 93, p. 103718, 2020.

[38] M. A. Abdullah, T. Al-Hadhrami, C. W. Tan, and A. H. Yatim, "Towards green energy for smart cities: particle swarm optimization based mppt approach," IEEE Access, vol. 6, pp. 58 427–58 438, 2018.

[39] G. Zhuo, J. D. Hostettler, P. Gu, and X. Wang, "Robust sliding mode control of permanent magnet synchronous generator-based wind energy conversion systems," Sustainability, vol. 8, no. 12, p. 1265, 2016.

[40] A.-R. Youssef, A. I. Ali, M. S. Saeed, and E. E. Mohamed, "Advanced multi-sector p&o maximum power point tracking technique for wind energy conversion system," International Journal of Electrical Power & Energy Systems, vol. 107, pp. 89–97, 2019.

[41] M. Qais, H. M. Hasanien, and S. Alghuwainem, "Salp swarm algorithm-based ts-flcs for mppt and fault ride-through capability enhancement of wind generators," ISA transactions, vol. 101, pp. 211–224, 2020.

[42] Z. A. Alrowaili, M. M. Ali, A. Youssef, H. H. Mousa, A. S. Ali, G. T. Abdel-Jaber, M. Ezzeldien, and F. Gami, "Robust adaptive hcs mppt algorithm-based wind generation system using model reference adaptive control," Sensors, vol. 21, no. 15, p. 5187, 2021.

[43] S. D. Ahmed, F. S. Al-Ismail, M. Shafiullah, F. A. Al-Sulaiman, and I. M. El-Amin, "Grid integration challenges of wind energy: A review," IEEE Access, vol. 8, pp. 10 857–10 878, 2020.

[44] H. H. Mousa, A.-R. Youssef, I. Hamdan, M. Ahamed, and E. E. Mohamed, "Performance assessment of robust p&o algorithm using optimal hypothetical position of generator speed," IEEE Access, vol. 9, pp. 30 469–30 485, 2021.

[45] M. Fannakh, M. L. Elhafyani, S. Zouggar, and H. Zahboune, "Performances mppt enhancement in pmsg wind turbine system using fuzzy logic control," in International Conference on Electronic Engineering and Renewable Energy. Springer, 2020, pp. 797–807.

[46] D. Zouheyr, B. Lotfi, and B. Abdelmadjid, "Improved hardware implementation of a tsr based mppt algorithm for a low cost connected wind turbine emulator under unbalanced wind speeds," Energy, p. 121039, 2021.
[47] S. Mirjalili, S. M. Mirjalili, and A. Lewis, "Grey wolf optimizer," Advances in engineering software, vol. 69, pp. 46–61, 2014.
[48] J. Kennedy and R. Eberhart, "Particle swarm optimization," in Proceedings of ICNN'95-international conference on neural networks, vol. 4. IEEE, 1995, pp. 1942–1948.
[49] A. P. Piotrowski, J. J. Napiorkowski, and A. E. Piotrowska, "Population size in particle swarm optimization," Swarm and Evolutionary Computation, vol. 58, p. 100718, 2020.
[50] A. Raza, Z. Yousaf, M. Jamil, S. O. Gilani, G. Abbas, M. Uzair, S. Shaheen, A. Benrabah, and F. Li, "Multi-objective optimization of vsc stations in multi-terminal vsc-hvdc grids, based on pso," IEEE Access, vol. 6, pp. 62 995–63 004, 2018.

HUSSEIN SHUTARI , received his B.Sc. degree in electronics and communications engineering from Faculty of Engineering, Hadhramout University, Yemen, in 2012, and the M.Sc. degree in electrical power system engineering from School of Electrical System Engineering, University Malaysia Perlis, Malaysia, in 2018. He is currently pursuing Ph.D. degree in electrical engineering at the Universiti Teknologi PETRONAS, Malaysia. His research interests include renewable energy systems operation, control, optimization and MPPT techniques for renewable energy systems.

DR. NORDIN SAAD is an Associate Professor in the Department of Electrical & Electronics Engineering at Universiti Teknologi PETRONAS, Malaysia. He was Head of the Department of Electrical & Electronics Engineering at the university from 1998 to 2000. He was cluster leader of the Industrial Automation and Control from 2005 to 2012, and subsequently co-cluster leader of the Power-Control and Instrumentation from 2013 to 2014. In addition he was a focal person for Group Technology Solution PETRONAS SKG 14 (Instrument) from 2006 until 2014, and more recently served as cluster leader for the Centre of Smart Grid Energy Research leading a group of ten active researchers. He received a BSEE degree from Kansas State University (USA), a M.Sc. in power electronics from Loughborough University (UK) and a Ph.D. in control engineering from The University of Sheffield (UK). His research areas include smart grids, renewable energy and energy systems, modern transportation systems, networked and industrial wireless communication, and smart fields. His current research work encompasses some of the issues in electrical drives control, power electronic converters for high power transmissions and low-power applications, condition monitoring and diagnostic of machines, and instrumentation and control of facilities. A total of seven Ph.D. and four M.Sc. by research graduates that have graduated under his supervision. He has published over 150 journals, transactions, book chapters and technical papers in these areas. He has authored and co-authored a total of four books. He is a Chartered Engineer, a senior member of IEEE (SMIEEE) and a member of the Institute of Measurement and Control (MInstMC) UK.

DR. NURSYARIZAL MOHD NOR obtained his PhD in Electrical Engineering from the Universiti Teknologi PETRONAS (UTP), Malaysia in 2009. In 2001 he obtained his M.Sc. in Electrical Power Engineering from The University of Manchester Institute of Science and Technology (UMIST), UK. His areas of specialization are 'Analysis and optimization of large scale power systems' and 'State estimation'. He has several publications at his credit. His research interests are in Power System State Estimation, Power System Analysis, Renewable Energy and Electrical Machine.

DR. MOHAMMAD FARIDUN NAIM TAJUDDIN received his B. Eng. and M. Eng. from the University of Malaya (UM), Malaysia in 2004 and 2007 respectively, and the Ph.D. degree from the Universiti Teknologi Malaysia (UTM), Johor, Malaysia in 2015. He is currently an Associate Professor with the Faculty of Electrical Engineering Technology, Universiti Malaysia Perlis (UniMAP). He has published refereed manuscripts in various reputable international journals. He also acts as a reviewer for various reputed journals, such as the IEEE, Elsevier Applied Energy, Renewable and Sustainable Energy Reviews, Neurocomputing and Energy Reports. His research interests include power electronics control, photovoltaic modeling and control, intelligent control and optimization techniques.

ALAWI ALQUSHAIBI received his B.Sc. degree in computer networks and security from Universiti Teknologi Malaysia, in 2012, and the M.Sc. degree in Information Technology (by research) from Universiti Teknologi PETRONAS. He is currently pursuing the Ph.D. in Information Technology with Universiti Teknologi PETRONAS. His research interests include machine learning and data science, specifically in deep learning optimization.

DR. MUAWIA ABDELKAFI MAGZOUB received a BSc. degree in Electrical Engineering from Al-Zaim Al-Azhari University, Khartoum, Sudan in 2005 and a Master's degree in Electronics Engineering from Sudan University of Science and Technology, Khartoum, Sudan in 2008 and a Ph.D. degree in Electrical and Electronics Engineering from the Universiti Teknologi PETRONAS, Malaysia in 2017. He worked as a lecturer at Al-Jraif Sharq Technical College, Khartoum, Sudan and served as a Senior Engineer in the Department of Tooling and Automation at Finisar II-VI (M) Sdn Bhd in Malaysia for two years and eight months. He is currently a Postdoctoral researcher with the Department of Electrical and Electronics Engineering, Universiti Teknologi PETRONAS, Malaysia. His main research areas are in the automation and process control, power electronics and machines control and machines applications, artificial intelligence, machine learning and data analysis.